NASA Technical Memorandum 102517

Use of Unbalanced Laminates as a Screening Method for Microcracking

Demetrios S. Papadopoulos
Case Western Reserve University
Cleveland, Ohio

and

Kenneth J. Bowles
Lewis Research Center
Cleveland, Ohio

Prepared for the
35th International SAMPE Symposium
Anaheim, California, April 2–5, 1990

NASA

USE OF UNBALANCED LAMINATES AS A SCREENING METHOD FOR MICROCRACKING

Demetrios S. Papadopoulos
Case Western Reserve University
Cleveland, Ohio 44106

and

Kenneth J. Bowles
National Aeronautics and Space Administration
Lewis Research Center
Cleveland, Ohio 44135

E-5214

SUMMARY

State-of-the-art, high temperature polyimide matrix composites, reinforced with continuous graphite fibers are known to be susceptible to intraply cracking when thermally cycled over their useful service temperature range. It is believed that the transply cracking, in part, results from residual stresses caused by differences in coefficients of thermal expansion (CTE) between the polymer matrix and the reinforcement. Thermal cycling tests to investigate this phenomenon involve expensive time and energy consuming programs which are not economically feasible for use as a part of a materials screening process.

As an alternative to thermal cycling studies, a study of unbalanced cross-ply graphite fiber reinforcement composites was conducted to assess the effect of the composite ply layup and surface condition on the residual stresses that remain after the processing of these materials. The residual stresses were assessed by measuring the radii of curvature of the types of laminates that were studied. The temperature at which stress-free conditions existed were determined and a dye penetrant method was used to observe surface damage resulting from excessive residual stress buildup. These results are compared with some published results of thermal cycling tests that were previously conducted on balanced polyimide composites.

INTRODUCTION

Aircraft engine materials forecasts for the decade of the 1990's and the early 21st century specify polymer matrix composites for use in aircraft engines and other high temperature structures with use temperatures as high as 427 °C. Current state-of-the-art high temperature composites are now limited to graphite fiber reinforced polyimides (such as PMR-15) materials. These materials are acceptable for engine use at 288 °C for times up to 5000 hr. The polyimide composites are processed at 316 °C and this level of temperature causes problems due to the residual stresses that are set up during the cool down to room temperature after the forming and curing step in the laminate processing have been completed. This type of behavior may be more severe with 427 °C composites.

The mismatch between the coefficients of thermal expansion of the graphite fiber (-1.0 to 10.0×10^{-6} $°C^{-1}$) and the polyimide matrix (56×10^{-6} $°C^{-1}$) creates a considerable amount of residual stresses within the composite as it is cooled

from the cure temperature to room temperature (a range of 290 °C). Depending upon the ply layup, these residual stresses may be severe enough to cause intralaminar cracks to develop during the cooling phase of processing. While the cracks may be suppressed initially, it was found that thermal cycling can induce these intraply cracks within the laminate (ref. 1). This type of damage is commonly referred to as microcracking. These microcracks can cause the degradation of matrix dominated mechanical properties and reduced structure life at elevated temperatures.

Aircraft engine structures made from polyimide composites, normally see temperatures from -60 to 288 °C. In order to conduct tests similar to these conditions, specialized thermal cycling equipment is required. Typical thermal cycling tests require days and weeks to complete. Thus, it would be very useful to develop a reliable, quick procedure to screen materials and rank them in their ability to resist microcracking. One obvious method for consideration would be the testing of unbalanced composites. Unbalanced composites have been used to measure residual strains caused by CTE differences between the crossplies (ref. 1). It would be expected that these strains can be related to thermal cycling induced intralaminar cracking (refs. 2 to 4).

In the work reported herein, the technique of using crossplied, unbalanced polymer matrix composites was used to assess residual stresses for a number of composite designs, layups and materials. Residual stresses were calculated for the different laminates using simple laminate theory. The composite designs that were studied were those that were believed to influence residual strain buildup (refs. 5 and 6). Celion 6000 and the higher strength AS4 were the two fibers that were included in this study. Three types of resins were included - PMR-15, PMR-II-50 and PEEK. The ply layups were limited to [0°, 90°]. The curvatures were measured after cool down, and the surfaces were photographed after treatment with a dye penetrant to visually high light surface damage that might be caused by the residual strains. The stress-free temperatures of the various composites were measured in an environmental chamber using a cathetometer such as that used in creep test measurements.

The composite designs were assessed on the basis of their radius of curvature and the crack density at the surfaces of the composites. The behavior of some composites were compared to similar composites that were thermally cycled by other investigators.

MATERIAL AND FABRICATION

The AS4/PEEK unbalanced laminates were purchased from Fiberite Corp. The PMR-15 matrix resin was prepared from the monomethylester of 5-norbornene-2,3-dicarboxylic acid (NE), 4,4'-methylenedianiline (MDA), and freshly esterified 3,3',4,4'-benzophenonetetracarboxylic acid (BTDA). These materials were obtained from commercial sources. The details of the esterification of the BTDA is given in reference 7. The preparation of PMR-II-50 resin is similar to that of PMR-15 except that the diester that was used was the dimethylester of 4,4' hexafluoroisopropylidinebis (phthalic acid) (HFDE), and the diamine was p-phenylenediamine (PPDA). The cure temperature was 316° for the PMR-15 composites and 371 °C for the PMR-II-50 composites. The details of the synthesis are given in reference 8.

The unsized AS4 fiber that was used was purchased from Hercules. Unsized Celion 6000 graphite fiber was purchased from BSAF. Typical properties of these two fibers are presented in table I. The mat material that was used in the compression molding of the Celion 6000/PMR-15 [0,90], mat laminate was purchased from the International Paper Company. The mat density was 0.2 oz/yd^2.

The following steps were employed in prepregging and laminate fabrication:

(1) fiber tow winding
(2) tow impregnation by the monomer solution
(3) drying
(4) ply cutting and layup
(5) imidization
(6) compression molding

This procedure is fully described elsewhere (refs. 7 and 8). A free standing postcure in air at 316 °C for 16 hr for the PMR-15 composites and 385 °C for the PMR-II-50 matrix composites was performed.

A series of six laminates were fabricated using Celion 6000 fibers as reinforcement. The laminates are described as follows:

(1) 0,90 (PMR-15)
(2) 0,0,90,90 (PMR-15)
(3) 0,90,mat (PMR-15)
(4) 0,90,resin (PMR-15)
(5) 0,90,0,90 (PMR-15)
(6) 0,90 (PMR-II-50)

In addition to these, one AS4/PEEK [0,90] and one AS4/PMR-15 [0,90] composites were examined. All laminates measured 20.3 by 7.6 cm.

TEST PROCEDURE

Upon removal from the matched metal die molds, the cured laminates warped into a cylindrical shape. The dimensions of the laminates were measured and the radii of curvature were calculated using the relationship:

$$r = \frac{\left(\frac{s}{2}\right)^2 + h^2}{2h} \qquad (1)$$

where r is the radius of curvature, s is the chord length and h is the arc height (fig. 1). The x, y, and z axes correspond to the 1, 2, and 3 axes of the laminate, respectively.

The stress free temperature of each laminate was measured. The stress free temperature is that temperature at which the radius of curvature of a laminate becomes infinite. The procedure involved the placement of each laminate within an Instron environmental chamber and heating it in steps of 50 °C to a temperature exceeding the cure temperature. The height, h, was measured with a cathetometer after equilibrium was reached at each temperature. The laminates stayed circular throughout the test, and radii of curvature were calculated from these data at each temperature.

The face of each laminate was treated with a dye-penetrant so that the stress cracks in the surface could be observed visually. The crack densities were measured as the number of cracks per unit length. The surfaces were then photographed showing the crack direction parallel to the fibers.

Using an H_2SO_4/H_2O_2 digestion technique (ASTM D-3171), the fiber contents of the laminates were measured. Composite densities were measured by the immersion method described in ASTM D-792. Flexural moduli of neat resins PMR-15, PMR II-50, unidirectional composites of 0° and 90° fiber orientation and also a fiber mat/PMR-15 composite were measured using the method specified in ASTM D-790. The glass transition temperature was measured by thermomechanical analysis (TMA).

EXPERIMENTAL RESULTS

The dimensional data for each laminate that was studied are presented in table II. These data were measured when the laminates were removed from the mold after the cure was completed. These data include length, width, thickness, arc height (h), chord length (s), and fiber volume percent. The fiber volume percent was measured after the stress free temperature was measured. In figure 2, the data have been reduced using equation (1), to give values of the room temperature radius of curvature for each laminate in both the longitudinal and transverse directions. Table III also contains the stress free temperatures and glass transition temperatures. Figure 3 shows a plot of the radius of curvature for each of the laminates as a function of temperature.

Figures 4 to 7 show the crack densities that were highlighted by dye penetrant examination of the laminates. The photographs were chosen to show differences due to variations in matrix, fiber and surface condition (mat and resin rich). Flexural strength and flexural moduli were measured on thicker unidirectional laminates in both the longitudinal and transverse directions. These measurements were made with Celion 6000/PMR-15, AS4/PEEK, AS4/PMR-15, mat/PMR-15, and Celion 6000/PMR-II-50 specimens. The results are presented in table IV.

DISCUSSION

When the unbalanced composites were removed from the mold after curing, they displayed two distinct radii of curvature, oriented perpendicular to each other. In most cases, the laminates could be snapped from one radius of curvature to the other. The exception to this was the AS4/PMR-15 [0,90]. This laminate was unstable in the secondary position because of insufficient residual stresses that were needed to maintain the shape. If the residual stresses do not exceed the elastic limit of the matrix, (thus causing matrix microcracking), the radii of curvature can be used as a measure of the developed matrix stress. It was found that the calculated strains were most severe near the edges and center of the laminate (figs. 9 and 10). This was confirmed by the crack patterns obtained by the dye penetrant. The strains range from a maximum tensile strain of 0.77 percent in the AS4/PEEK system to -1.14 percent compressive strain in the AS4/PEEK system. The midplane strains were obtained from the equations:

$$e_x^o = a_1 + a_2x^2 - \frac{aby^2}{4} \tag{2}$$

$$e_y^o = b_1 + b_2y^2 - \frac{aby^2}{4} \tag{3}$$

$$e_{xy}^o = 0 \tag{4}$$

where a_1, a_2, b_1, b_2 are constants calculated from laminate theory (ref. 4). The constants a and b were determined from laminate geometry (fig. 1). Since the laminates curled into cylindrical shapes after the cure, b = 0 when the laminate curled about the 90° axis and a = 0 when the laminate was curled about the 0° axis. Thus, the equations simplify to:

$$e_x^o = a_1 + a_2x^2 \tag{5}$$

$$e_y^o = b_1 + b_2y^2 \tag{6}$$

$$e_{xy}^o = 0 \tag{7}$$

Since the constants a_1, a_2, b_1, and b_2 in the equations are based on laminate geometry, the calculated strains are a measure of residual strain in the laminate after cracking has occurred.

For convenience and simplification of data presentation, the materials that were studied were divided into two groups. One group contains composites with different matrix and fiber reinforcement materials. The second group contains those composites with different surfaces and ply layup sequences. The Celion 6000/PMR-15 [0,90] composite is the control reference for both sets of composites. In interpreting the experimental results, small radii of curvature and/or high crack densities indicate the presence of high residual stresses that develop during the cooling of the laminates from the cure temperature to room temperature. Both parameters must be considered since an increase in crack density will cause a corresponding increase in radius of curvature due to the resultant relief of residual stresses.

Variations in matrix material and reinforcement fiber did result in significant differences in the room temperature physical and dimensional condition of the unbalanced composites that were studied. Comparisons of the cured composites can be summarized as follows:

Radius of curvature and crack density. - A comparison of the four composites with different reinforcements and matrices (figs. 2(b) and 8(b)) show that the AS4/PEEK composite possessed the lowest crack density and also the lowest radius of curvature. The combination indicates a composite toughness that is greater than the control specimen. The PEEK neat resin has a room temperature strain at failure in excess of 40 percent (refs. 9 and 10). The AS4/PMR-15 has a slightly lower crack density than the control material but it is not a significant difference. The greater radius of curvature in comparison to that of

the control, coupled with the very slight difference in crack densities, suggest a lower level of residual stresses within the AS4/PMR-15 laminate but not necessarily a greater toughness. The Celion 6000/PMR II-50 specimen exhibited the greatest differences in crack density and radius of curvature when compared with the control material. The crack density is the highest of all the laminates that were tested in this study. For this particular laminate, the cracking process continued slowly and sporadically as time elapsed. Eventually the laminate flattened out as the crack density became large enough to relieve all the residual stresses. The crack distribution is relatively uniform as shown in figure 6. These conditions suggest that very high residual strains developed within the laminate during cool down or that the strain at failure is less than that of the PMR-15. This will be examined later.

Comparison of the three different ply layup sequences (figs. 2(a) and 8(a)) indicate that the thin, two ply layup is the most sensitive to the formation of transply cracks from residual matrix strains in unbalanced composites. A comparison of the [0,90] layup with the [0,0,90,90] layup in effect compares ply thickness effects. The [0,0,90,90] is a two ply unbalanced composite with each ply being twice as thick as corresponding ply in the [0,90] laminate. For the unbalanced composites, thinner surface plies are more susceptible to intraply cracking than thicker plies. The [0,90,0,90] laminate was included to provide unbalanced conditions between those of the thin, two ply composite and a completely balanced composite. As expected, the absence of cracks and the very large radius of curvature values show that this ply layup design is not sensitive to crack formation.

CTE and flexural properties. - (Tables IV and V) The data in table V show that the CTE's are different for the three matrix resins and their composites. The CTE's for PMR-II-50 and Celion 6000/PMR-II-50 are higher than the values for the corresponding PMR-15 materials. This reflects the lower crosslink density in the PMR-II-50 which has an average prepolymer molecular weight of 5000 in comparison to 1500 for PMR-15. The measured stress free temperature for PMR-II-50 is 342 °C, 23 °C lower than that of the PMR-15. This also reflects the differences in the crosslink densities. The difference in the CTE values measured across the fibers (90° direction) produce a residual stress increase of about 0.23 percent in the PMR-II-50 composite in relation to that in the PMR-15 composite. It appears that the low transply crack resistance of the Celion 6000/PMR-II-50 can be attributed to the higher CTE in reference to the control. The matrix material PEEK exhibited the lowest average CTE of the resins tested, yet had the highest average CTE across the fibers in the composite. The low crack density in the AS4/PEEK system probably results from the high strain to failure of PEEK and the possible relaxation of stresses due to the semicrystalline nature of the matrix.

The CTE of the mat material more closely matches that of the CTE parallel to the fiber axis. Thus, the mismatch between the mat surface and the underlying ply is much less than between plies in the control specimen. The addition of the mat layer caused a very small increase in the radii of curvature of the test laminate, which is probably not significant because of measurement error effects in the radius of curvature equation (see Error Analysis). In addition to the effect of the small CTE of the mat material, the randomly oriented short fibers present no direct path for crack growth through the surface layer, and the surface layer has a greater strength and modulus than the 90° surface of the control (table IV).

The resin rich surface significantly reduced the crack density on the 90° fiber surface of the test laminate (fig. 4(a)). This type of surface also caused a reduction in the radius of curvature about the 90° axis and an increase about the 0° axis. The changes in the radii are due to the increase in CTE of the resin rich surface layer which resulted in a greater contraction of the surface. This surface also has a lower flexural modulus and a higher strength than the 90° ply of the control specimen. The flexural strain at failure is about two to three times that of the composite. The surface flexural properties probably influence the crack resistance significantly.

Stress free temperature. - The stress free temperature was determined by measuring the temperature when the laminates became flat. As shown in figures 3(a) and (b), the radius of curvature gradually increased while below the cure temperature (316 °C). When the cure temperature was reached, the rate of increase of radius of curvature then increased. In most cases the stress free temperature was not at the cure temperature, but at or above the glass transition temperature (table III). It is evident that the stress free temperatures range from Tg to temperatures as high as 35 °C above Tg. This is not in agreement with Kim, et al. (ref. 6) who measured stress free temperatures at the matrix Tg for the AS4/PEEK system. During cool down, the laminate's radius of curvature plot retraced itself showing no traces of hysteresis, thus eliminating evidence of further crosslinking and increased residual stresses which would be observed as a tighter radius of curvature of the laminate.

ERROR ANALYSIS

All dimensional measurements performed on the laminates were made to ±0.01 cm except for the thickness dimension which was measured to 0.0001 cm. The effect of this deviation on the radius of curvature (eq. (1)) is as follows:

$$dr = \frac{\partial r}{\partial s} ds + \frac{\partial r}{\partial h} dh$$

$$= \frac{s}{4h} ds + \left(0.5 - \frac{s^2}{8h^2}\right) dh \qquad (8)$$

The worst case was with $s = 20.27$ cm and $h = 0.90$ cm with ds and dh of opposite signs. Taking $dh = -0.01$ cm and $ds = 0.01$ cm:

$$dr = \frac{(20.27)(0.01)}{4(0.90)} + \left(0.5 - \frac{20.27^2}{8(0.90)^2}\right)(-0.01)$$

$$= 0.69 \text{ cm}$$

Due to dimensional measurement, the radius of curvature can vary by ±0.69 cm.

The composition of each laminate across its cross section was fairly uniform with respect to fiber volume ratio. The fiber volume ratios had a standard deviation that ranged from 0.1 to 5.5 percent. However, the standard deviations for the crack densities of the unbalanced laminates ranged from 30 to 100 percent of the average crack density value. These high standard

deviations result from the nonuniformity of the crack patterns on the laminate surfaces. Cracked areas formed in clusters around stress concentrations on the surface of the laminate. Alternating areas of high crack density and low crack density or no cracks created the high standard deviation values.

From a thermal analysis standpoint, the CTE typically displayed standard deviations between 10 and 35 percent of the average value over the temperature range of 0 to 350 °C for the 90° directions, mat composite, and resin specimens. The standard deviations of the CTE in the 0° direction were on the order of magnitude of the mean value of the measurements because the minor perturbation in the slope of the TMA curve have a larger impact on the numerically small mean. Both the stress free and glass transition temperatures were measured to ±1 °C.

The mechanical properties exhibited low standard deviations of 2 to 5 percent of the reported value. The exception to this was the AS4/PMR-15 [0,90] composite which has standard deviations of 8 to 12 percent of the reported values.

SUMMARY OF RESULTS

PMR-15 composites, made at the NASA Lewis Research Center from [0,90] Celion 6000 fabric plies, were shipped to Rohr Industries for thermal cycling tests under a previous program. The laminates included PMR-15 as a control, a laminate with mat surfaces and four laminates with varying fiber volume fractions. The results of these tests suggest that the mat surfaces and a decrease in fiber content reduce the microcrack formation from exposure to 1000 thermal cycles over the temperature range of -18 to 232 °C (table VI). The resin rich laminate in this study has two different fiber volume fractions on the two surfaces of the specimen. The surface with the lower fiber content experienced less cracking than the surface with greater fiber content and also the control specimen. In general the results of the two separate tests indicate an agreement between thermal cycling results and unbalanced composite data under the conditions described above.

From the results of this study, the use of unbalanced composites as a screening test for rating the microcracking resistance of composites looks promising. Further study is necessary to determine the degree of applicability of using unbalanced composites as a means for screening materials for thermal cycling damage resistance. Recommendations for further study are: fiber content, matrix strain to failure, and actual comparison with thermal cycled composites.

CONCLUSIONS

As shown in table VI, the surface conditions of the laminate effect the severity of cracking and the extent of crack propagation. In addition, the reduced crack densities on the mat surface and resin surface laminates also correlate with thermocycling data from General Electric and DuPont (refs. 5 and 11). The results of these experiments can give a qualitative indication of microcracking resistance of different surface treatments and fiber/matrix combinations.

REFERENCES

1. G.A. Owens, and S.E. Schofield, "Thermal Cycling and Mechanical Property Assessment of Carbon Fibre Fabric Reinforced PMR-15 Polyimide Laminates," Compos. Sci. Technol., 33, (1988), 177-190.

2. H. Dannenberg, "Determination of Stresses in Cured Epoxy Resin Composites," SPIE J., 21, (1965), 669-675.

3. J.P. Favre, "Residual Thermal Stresses in Fiber Reinforced Materials--A Review," J. Mech. Behav. Mater., 1, (1988), 37-53.

4. M.W. Hyer, "The Room-Temperature Shapes of Four-Layer Unsymmetric Cross-Ply Laminates," J. Compos. Mater., 16, (1982), 318-340.

5. H.Y. Loken, and J.L. Cooper, "Water Ingression Resistant Thin Faced Honeycomb Cored Composite Systems with Facesheets Reinforced with KEVLAR Aramid Fiber or KEVLAR with Carbon Fibers," Composites '86: Recent Advances in Japan and the United States, K. Kawata, V. Sokichi, and A. Kobayshi, eds., Japan Society for Composite Materials, Tokyo, Japan, (1986).

6. K.S. Kim, H.T. Hahn, and R.B. Croman, "The Effect of Cooling Rate on Residual Stress in a Thermoplastic Composite," J. Compos. Technol. Res., 11, (1989), 47-52.

7. R.D. Vannucci, and D. Cifani, "The 700 °F Properties of Autoclave Cured PMR-II Composites," NASA TM-100923 (1988), p. 3.

8. R.D. Vannucci, "PMR-15 Polymide Modifications for Improved Prepreg Task," National Technical Conference: The Plastics ABC's: Polymer Alloys, Blends and Composites, Society of Plastic Engineers, (1982), pp. 131-133.

9. O.B. Searle, and R.H. Pfeiffer, "Victrex (R) Poly(ethersulfone) (PES) and Victrex Poly(etherether ketone) (PEEK)," Poly. Eng. Sci., 25, (1985), 474-476.

10. Materials Selector 1985, Penton/IPC, Cleveland, OH (1985), pp. 3-22.

11. D. Ward, Private conversation, General Electric Company, Evendale, OH, Oct. 27, 1989.

12. ICI Fiberite Data Sheet 3a.

TABLE I. - PROPERTIES OF THE REINFORCING FIBERS

	Celion 6000[a]	AS4[b]
Tensile strength, Mpa (ksi)	3240 (470)	3795 (550)
Tensile modulus, GPa (Msi)	234 (34)	234 (34)
Ultimate elongation, percent	1.54	1.53
Density, g/cm^3 (lb/in.^{3})	1.77 (0.064)	1.80 (0.065)

[a]Data obtained from Celanese Structural Composites.
[b]Data obtained from Hercules Incorporated.

TABLE II. - LAMINATE PROPERTIES

Laminate	Length, cm	Width, cm	Thickness, cm	Fiber volume, percent	Longitudinal		Transverse	
					Chord	Arc height, cm	Chord	Arc height, cm
Celion 6000/PMR-15 0,90	20.40	7.65	0.0381	67.2	12.00	6.86	7.30	0.98
Celion 6000/PMR-15 0,90,Mat	20.40	7.65	.0381	60.5	13.05	6.45	7.40	.80
Celion 6000/PMR-15 0,90,Resin	20.40	7.65	.0457	52.9	7.65	7.49	7.53	.38
Celion 6000/PMR-15 0,0,90,90	20.40	7.66	.0762	58.2	18.35	3.81	7.54	.45
Celion 6000/PMR-15 0,90,0,90	20.42	7.66	.0813	69.0	20.27	.90	7.65	.10
AS4/PMR-15 0,90	20.41	7.60	.0508	73.4	Unstable		7.47	.79
AS4/PEEK 0,90	20.09	7.49	.0282	66.9	(a)	(a)	6.91	1.42
Celion 6000/PMR-II-50 0,90	20.35	7.59	.0533	57.7	19.61	2.42	7.52	.84

[a]The radius of curvature was measured directly.

TABLE III. - STRESS FREE TEMPERATURES AND GLASS TRANSITION TEMPERATURES OF THE UNBALANCED LAMINATES

Laminate	Stress free temperature, °C	Glass transition temperature, °C
Celion 6000/PMR-15 [0,90]	365	330
Celion 6000/PMR-15 [0,90,0,90]	320	335
Celion 6000/PMR-15 [0,0,90,90]	352	335
Celion 6000/PMR-15 [0,90,Mat]	354	344
Celion 6000/PMR-15 [0,90,Resin]	357	358
Celion 6000/PMR II-50 [0,90]	342	338
AS4/PMR-15 [0,90]	348	328
AS-4/PEEK [0,90]	320	330

TABLE IV. - FLEXURAL PROPERTIES OF GRAPHITE REINFORCED COMPOSITES

Composite	Fiber Orientation							
	0°				90°			
	Modulus		Strength		Modulus		Strength	
	GPa	Msi	MPa	ksi	Gpa	Msi	MPa	ksi
Celion 6000/PMR-15	132	18.9	1948	278.9	9.6	1.38	84	12.1
AS4/PMR-15	116	16.6	1461	209.2	10.8	1.54	59	8.5
AS4/PEEK11	121	17.5	1880	273	8.9	1.29	137	19.9
Celion 6000/PMRII-50	124	17.7	1742	249.4	8.1	1.16	98	14.1
PMR-15 Resin	3.8	.55	103	14.8	----	----	---	----
PEEK9,10	2.6	.52	93	13.5	----	----	---	----
PMR-II-50	-----	-----	----	-----	----	----	---	----
Random Mat/PMR-15	14.5	2.10	279	40.4	----	----	---	----

TABLE V. - AVERAGE COEFFICIENT OF THERMAL EXPANSION ($\times 10^{-6}/°C$)[a]

Laminate	Direction	
	0°	90°
Celion 6000/PMR-15	-1.03	27.9
Mat/PMR-15	4.35	4.74
Celion 6000/PMR-II-50	-1.22	36.9
AS4/PMR-15	-3.24	28.8
AS4/PEEK	-1.47	[b]52.8
PMR-15	56.0	----
PMR-II-50	60.7	----
PEEK[9,10]	[c]47.0	----

[a]Average values from 20 to 300 °C.
[b]25.3 at 20 to 150 °C; 71.1 at 150 to 300 °C.
[c]108 above 150 °C.

TABLE VI. - THERMAL CYCLING OF Gr/PMR-15 LAMINATES

[1000 cycles; -18 to 232 °C.]

Laminate	Number of initial cracks (cracks/in.^{2})	Number of final cracks (cracks/in.^{2})
PMR-15, Control	0	58
PMR-15, Mat Surface		0
PMR-15, 59.88 percent fiber volume		50
PMR-15, 55.68 percent fiber volume		39
PMR-15, 52.50 percent fiber volume #1		22
#2		20

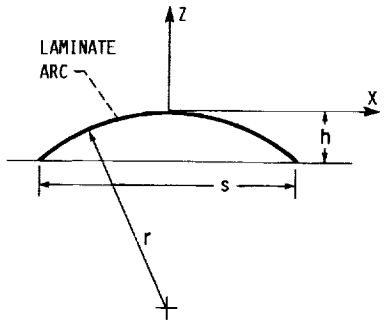

$z = \frac{1}{2}ax^2 + \frac{1}{2}by^2$ (REF. 4)

FOR:

$a = 0 \quad b = \frac{8h}{s^2}$

$b = 0 \quad a = \frac{8h}{s^2}$

FIGURE 1. - DETERMINATION OF RADIUS OF CURVATURE.

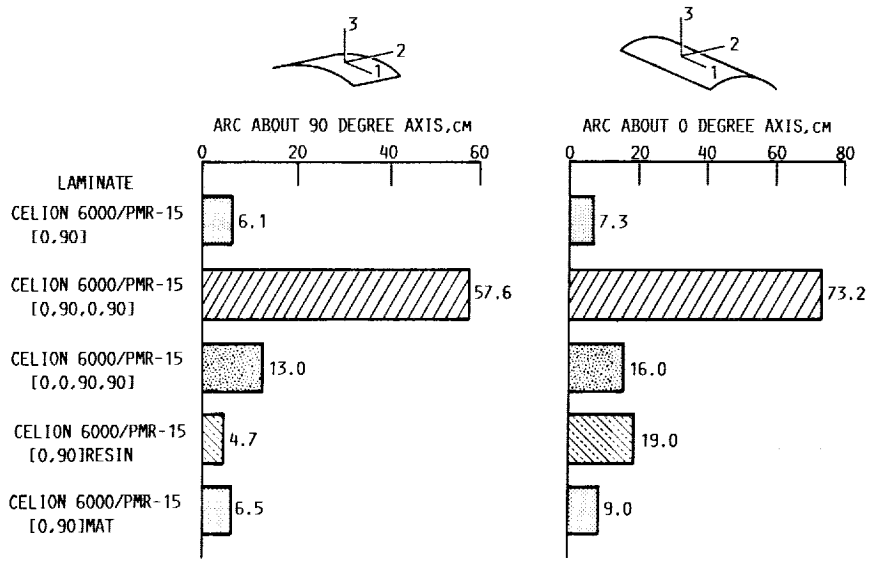

(a) PLY LAYUP AND SURFACE VARIATIONS.

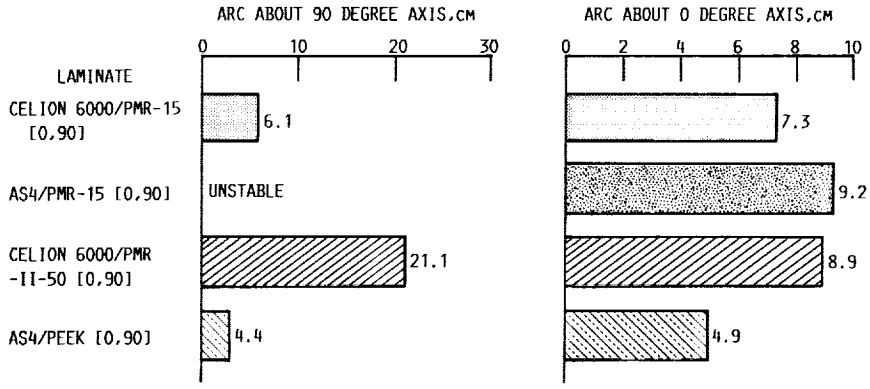

(b) CONSTITUENT VARIATIONS.

FIGURE 2. - RADIUS OF CURVATURE OF UNBALANCED LAMINATES.

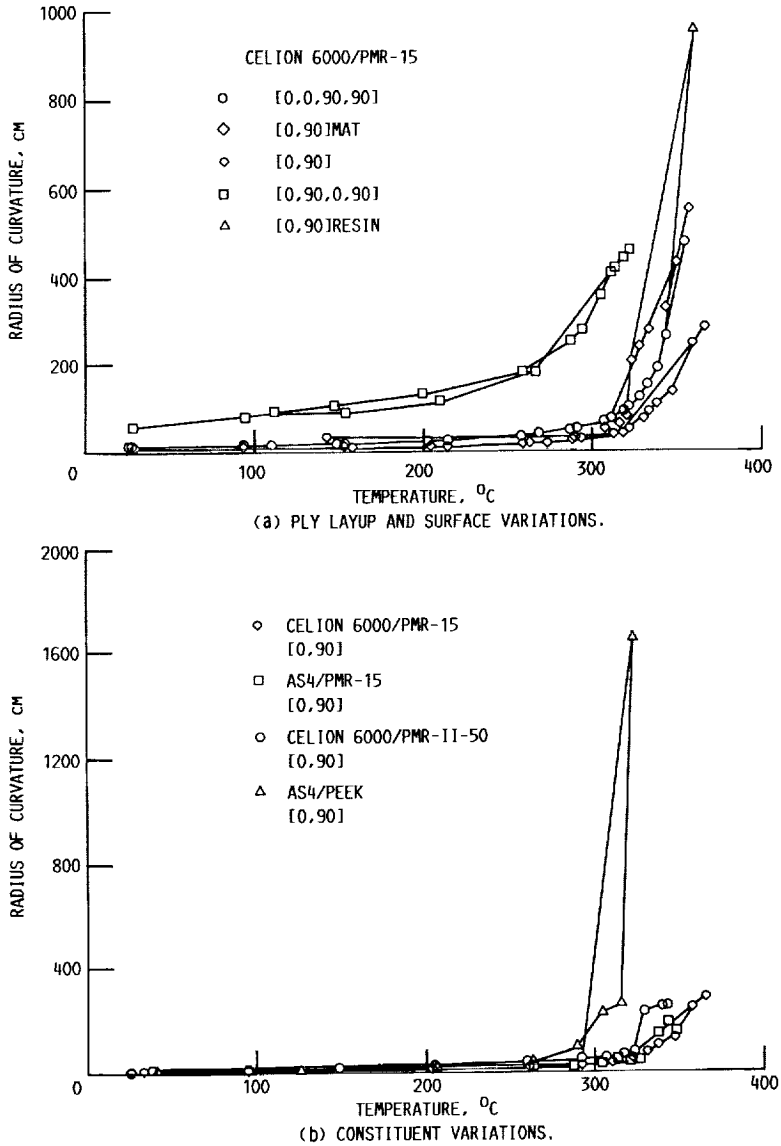

FIGURE 3. - RADIUS OF CURVATURE TO CENTER OF LAMINATE AS A FUNCTION OF TEMPERATURE.

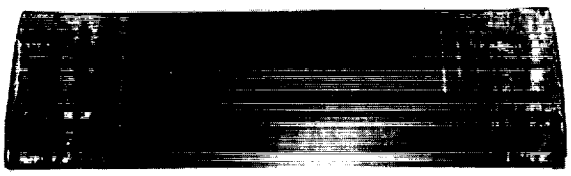

FIGURE 4. - CELION 6000/PMR-15 0,90 90^0 SIDE.

FIGURE 5. - CELION 6000/PMR-15 0,90,MAT MAT SIDE.

FIGURE 6. - CELION 6000/PMR-II-50 0,90 90^0 SIDE.

FIGURE 7. - AS4/PEEK 0,90 90^0 SIDE.

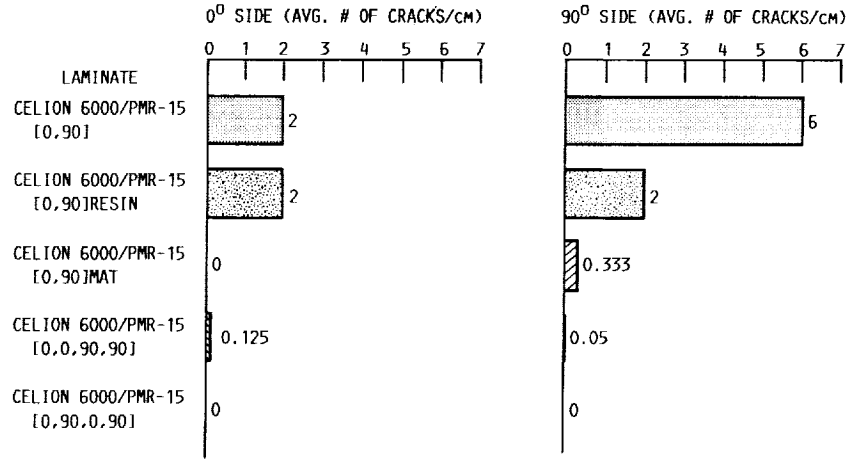

(a) PLY LAYUP AND SURFACE VARIATIONS.

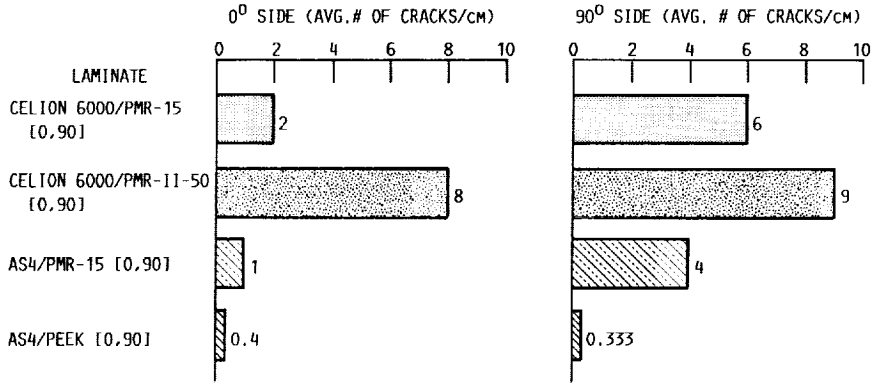

(b) CONSTITUENT VARIATIONS.

FIGURE 8. - NUMBER OF CRACKS PER CENTIMETER IN UNBALANCED LAMINATES.

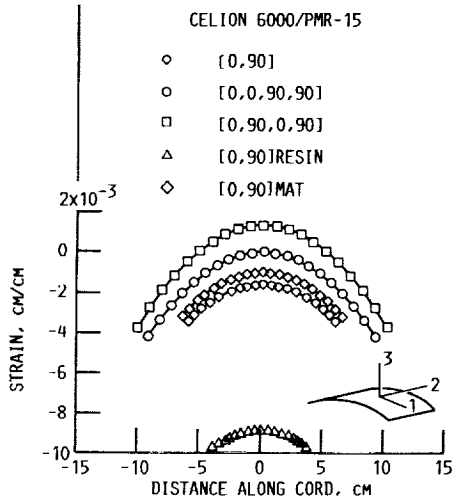

(a) LONGITUDINAL STRAIN FOR ARC ABOUT TRANSVERSE AXIS.

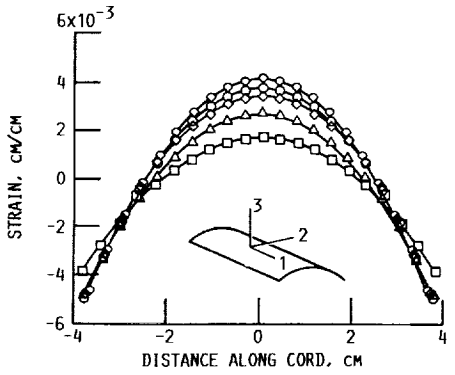

(b) TRANSVERSE STRAIN FOR ARC ABOUT LONGITUDINAL AXIS.

FIGURE 9. - MIDPLANE STRAIN vs DISTANCE ALONG ARC CORD.

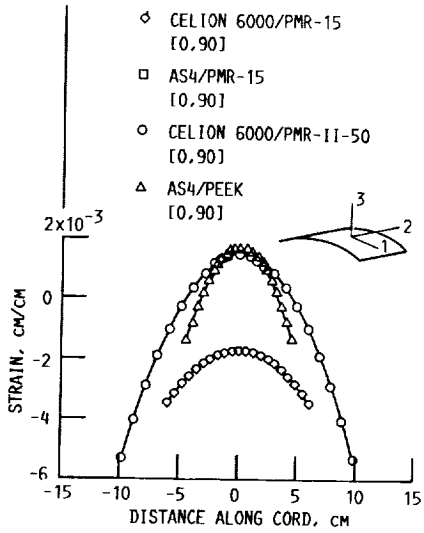

(a) LONGITUDINAL STRAIN FOR ARC ABOUT TRANSVERSE AXIS.

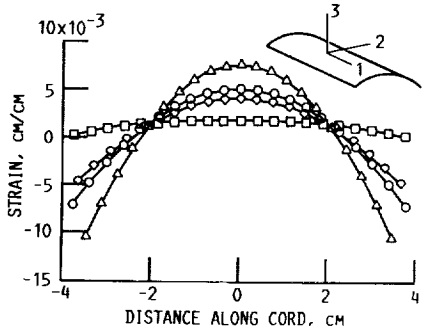

(b) TRANSVERSE STRAIN FOR ARC ABOUT LONGITUDINAL AXIS.

FIGURE 10. - MIDPLANE STRAIN vs DISTANCE ALONG ARC CORD.

NASA
National Aeronautics and Space Administration

Report Documentation Page

1. Report No.	2. Government Accession No.	3. Recipient's Catalog No.
NASA TM-102517		

4. Title and Subtitle	5. Report Date
Use of Unbalanced Laminates as a Screening Method for Microcracking	6. Performing Organization Code

7. Author(s)	8. Performing Organization Report No.
Demetrios S. Papadopoulos and Kenneth J. Bowles	E-5214
	10. Work Unit No. 510-01-0A

9. Performing Organization Name and Address	11. Contract or Grant No.
National Aeronautics and Space Administration Lewis Research Center Cleveland, Ohio 44135-3191	13. Type of Report and Period Covered Technical Memorandum

12. Sponsoring Agency Name and Address	14. Sponsoring Agency Code
National Aeronautics and Space Administration Washington, D.C. 20546-0001	

15. Supplementary Notes

Prepared for the 35th International SAMPE Symposium, Anaheim, California, April 2-5, 1990. Demetrios S. Papadopoulos, Case Western Reserve University, Cleveland, Ohio 44106; Kenneth J. Bowles, NASA Lewis Research Center.

16. Abstract

State-of-the-art, high temperature polyimide matrix composites, reinforced with continuous graphite fibers are known to be susceptible to intraply cracking when thermally cycled over their useful service temperature range. It is believed that the transply cracking, in part, results from residual stresses caused by differences in coefficients of thermal expansion (CTE) between the polymer matrix and the reinforcement. Thermal cycling tests to investigate this phenomenon involve expensive time and energy consuming programs which are not economically feasible for use as a part of a materials screening process. As an alternative to thermal cycling studies, a study of unbalanced crossply graphite fiber reinforcement composites was conducted to assess the effect of the composite ply layup and surface condition on the residual stresses that remain after the processing of these materials. The residual stresses were assessed by measuring the radii of curvature of the types of laminates that were studied. The temperature at which stress-free conditions existed were determined and a dye penetrant method was used to observe surface damage resulting from excessive residual stress buildup. These results are compared with some published results of thermal cycling tests that were previously conducted on balanced polyimide composites.

17. Key Words (Suggested by Author(s))	18. Distribution Statement
Polymer; Graphite fiber; Composites; Microcracking; Residual stresses; Coefficient of thermal expansion	Unclassified – Unlimited Subject Category 24

19. Security Classif. (of this report)	20. Security Classif. (of this page)	21. No. of pages	22. Price*
Unclassified	Unclassified	16	A03

*For sale by the National Technical Information Service, Springfield, Virginia 22161